

Influence of Boundary-Layer Transition on Measured Incipient Separation Angles

Donald Frew,* Lello Galassi,† and Donald Stava‡

U.S. Air Force Wright Laboratory, Wright–Patterson Air Force Base, Ohio 45433-7936
and

David Azevedo§

Pratt and Whitney, United Technologies, West Palm Beach, Florida 33410

The results of an investigation of shock-wave/turbulent boundary-layer interaction at nominal freestream Mach numbers between 5 and 6 are presented. This study examined the influence of boundary-layer transition on the two-dimensional incipient separation limit. The proximity of an externally generated shock/boundary-layer interaction to the end of flat-plate boundary-layer transition (defined as the peak heating location) was observed to have a first-order influence of the incipient separation angle. The interaction region needs to be located at least 50 boundary-layer thicknesses downstream of the peak heating location to avoid this influence. This finding is consistent with earlier reports found in the literature.

Nomenclature

- h = vertical distance between the shock-generator leading edge and the flat plate, Fig. 1
- h = convective heat transfer coefficient, Fig. 2
- L = length of flat plate
- M_∞ = freestream Mach number
- p = static pressure
- p_u = static pressure of undisturbed flow at shock location
- Re = Reynolds number
- St = Stanton number
- T_0 = total temperature
- U = velocity in x direction
- x = axial distance from leading edge of flat plate
- y = perpendicular height above the flat plate
- α = flat plate angle of attack
- δ = boundary-layer thickness
- θ = shock-generator angle
- θ_m = momentum thickness

Subscripts

- e = boundary-layer edge
- i = incipient separation angle
- s = inviscid shock impingement location
- tr = end of transition location
- w = shock-generator (i.e., wedge) leading-edge location relative to flat plate leading edge
- x = axial distance from leading edge of flat plate

Introduction

MOST of the shock-wave/boundary-layer interaction (SWBLI) data obtained during the 1950s and 1960s aided in the understanding of certain features of incipient

separation. However, inconsistencies among various experiments, as well as incomplete reporting of pertinent (in hindsight) test conditions, made difficult the development of accurate prediction tools for either incipient separation angle or incipient pressure rise. In particular, the dependence of turbulent incipient separation angle upon the locally defined Reynolds number Re_δ was left unresolved by these initial investigations.

A number of key technical papers,^{1–6} appearing from 1969 to 1976, when considered together, provide perhaps the best insight into the physics of the turbulent SWBLI and into the observed Re_δ trend. Together, they also describe most of the incipient separation measurement techniques employed. These references, with the exception of Holden,⁴ focused solely on the compression ramp configuration, due to its importance in relation to vehicle control surfaces. A detailed review of these papers is provided by Delery and Marvin.⁷ A concern raised by these investigators was whether a fully equilibrium turbulent boundary layer had been attained. Most of these references cited the work of Johnson and Bushnell,⁸ who found that the power-law exponent of flat-plate velocity profiles depends strongly on proximity to the end of boundary-layer transition (defined as the peak-heating point in the absence of a shock interaction). In particular, Johnson and Bushnell noted that a distance of 50δ downstream of this peak-heating point is required before one can consider the boundary layer to be fully turbulent.

The less-discussed impinging shock configurations are important as well, being directly related to the inlet design of high-speed flight vehicles, particularly mixed-compression inlet designs. More specifically, desirable high Mach ($M > 5$) operation of a ramjet or scramjet flowpath requires that the inlet shock strength be just below that for incipient separation of the bodyside boundary layer (to reduce the possibility of an unstart). Since one cannot, in general, duplicate all of the full-scale inlet flight parameters simultaneously (i.e., Mach number, turbulent boundary-layer characteristics, Re_δ , wall temperature) in existing ground-based facilities, extrapolation of small-scale model data is required. Thus, there is a need for carefully designed impinging shock tests for hypersonic Mach numbers.

The motivation for the present test program was to determine how the two-dimensional incipient separation angle is influenced by practical inlet design features. Our goal was to use the test data to develop a two- to three-dimensional meth-

Received Feb. 8, 1994; revision received Oct. 3, 1994; accepted for publication Oct. 29, 1994. This paper is declared a work of the U.S. Government and is not subject to copyright protection in the United States.

*Lieutenant, Aerospace Engineer, WL/FIMH Building 450, 2645 Fifth Street, Suite 30. Member AIAA.

†Captain, Aerospace Engineer, WL/FIMH Building 450, 2645 Fifth Street, Suite 30. Member AIAA.

‡Aerospace Engineer, WL/FIMH Building 450, 2645 Fifth Street, Suite 30.

§Senior Engineer, Hypersonics and Integration. Senior Member AIAA.

odology useful for ramjet and scramjet design activities. Such a methodology would identify the design parameters one should manipulate if inlet boundary-layer separation control is a primary concern, and might also allow the existing two-dimensional SWBLI database to be more fully utilized in the design phase, thus avoiding the need to perform expensive design-specific testing over a large parametric range. Most design-specific inlet rigs are rarely flexible enough to sort out the relative importance of individual contributions to incipient separation. The present authors are not aware of any systematic investigation that has related the two-dimensional SWBLI to practical three-dimensional inlet configurations, although Reda and Murphy^{9,10} have obtained some relevant data at Mach 2.9.

Although a number of parameters were examined in the present test program,¹¹ the most interesting empirical result (and the only one reported here) was that the relative location of the SWBLI to the boundary-layer transition endpoint greatly influenced the separation limit as detected by wall pressure taps. While we did not explore, in detail, the physics of this phenomenon, due to schedule constraints, we believe that this data is rather unique and worthy of further investigation.

Experiment

A synopsis of the test conditions, model description, and instrumentation is provided later in this article. A more complete description is included in Ref. 11.

Test Facility and Procedure

Tests were conducted at a nominal Mach number of 5.85 in an axisymmetric freejet blowdown-type tunnel with a stagnation pressure operating range of 0.69–13.8 MPa and total temperatures from 500 to 611 K.¹² Reynolds numbers for these conditions range from $4.9 \times 10^6 \text{ m}^{-1}$ to $98.4 \times 10^6 \text{ m}^{-1}$. All runs at $M = 5.85$ were conducted in the 4.9–13.8 MPa range ($Re = 34.1 \times 10^6 \text{ m}^{-1}$ to $97.4 \times 10^6 \text{ m}^{-1}$), at $T_0 = 556 \text{ K}$, this produced turbulent boundary layers in the SWBLI region. For $M = 5.07$, the unit Reynolds numbers behind the leading-edge shock-wave range from $45.9 \times 10^6 \text{ m}^{-1}$ to $131.6 \times 10^6 \text{ m}^{-1}$.

Model Description

The test employed a flat plate model, 46.99 cm long and 24.13 cm wide, which could be oriented at two angles of attack, $\alpha = 0 \text{ deg}$ ($M = 5.85$) and $\alpha = 6 \text{ deg}$ ($M = 5.07$ behind the leading-edge shock wave). An external shock-generating wedge driven by computer-controlled stepper motors provided the impinging shock wave. Figure 1 provides a sketch of the setup.

Shock generator angles could be controlled to within $\pm 0.1 \text{ deg}$. The wedge and plate were mounted independently so that the horizontal and vertical spacing between the leading edges of the plate and the wedge could be varied. In this manner, several shock impingement locations could be obtained for a given tunnel operating condition (in fact, horizontal spacing x_w could be varied during a run). Although sidewalls were employed for some runs in this test program, all results to be presented here were obtained without sidewalls.

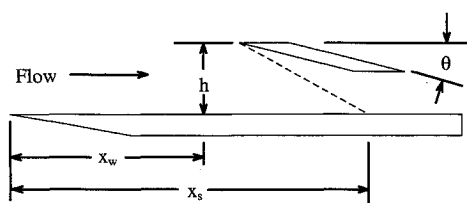


Fig. 1 Side view of flat plate/shock-generator model.

Instrumentation

The flat plate was instrumented with 66 pressure taps and 58 type E coaxial heat transfer gauges. The pressure taps in the SWBLI region were spaced 3.175 mm (approximately 0.58) apart along the model centerline, and were arranged in a chevron pattern to prevent tap-to-tap interference. A “kink” in the axial pressure distribution was the primary diagnostic for identifying boundary-layer separation. Spanwise rows of pressure taps aided in assessing flow uniformity. The measurement uncertainty was $\pm 0.07 \text{ kPa}$.

The heat transfer gauge spacing along the model centerline was 6.35 mm (approximately 1.08). Although this spacing did not allow as accurate an indication of incipient separation as the pressure taps, it did provide a consistent measure of the laminar-to-turbulent transition endpoints. Spanwise gauges provided a redundant means of assessing flow uniformity. The derived Stanton number uncertainty was $\pm 10\%$.

Boundary-layer measurements (pitot probe and total temperature probe) were made at selected axial stations, without the shock generator in place, to characterize the flow profiles. Schlieren video was taken for all runs as a secondary means of identifying boundary-layer separation, although the results to be presented are based solely on static pressure measurements. Although oil flow visualization was planned, these tests were not performed due to schedule constraints.

Pressure taps were also located on the shock generator, to verify angles and any shock reflected from the flat-plate surface for certain test conditions.

Results

Flat Plate, No Shock Generator

With the shock generator removed, the flat plate flow was characterized, for a variety of unit Reynolds numbers, in terms of where boundary-layer transition ended (defined as the peak heating point). In addition, boundary-layer profiles were measured at selected axial locations upstream, and within the expected SWBLI region.

From the Stanton number distributions shown in Fig. 2, it is seen that transition typically ended at a Reynolds number Re_x of about 12.0×10^6 for $M = 5.85$. Similar distributions for $M = 5.07$ indicate a common Re_x for transition end of 11.2×10^6 . The corresponding transition end locations x_{tr} are given in Table 1 and have an uncertainty of $\pm 2 \text{ cm}$. The tabular values in parentheses represent extrapolations from the measured points, as the most upstream heat transfer gauge was 15.24 cm from the leading edge of the model.

Typical boundary-layer velocity and total temperature profiles are shown in Fig. 3. The velocity profiles were used to

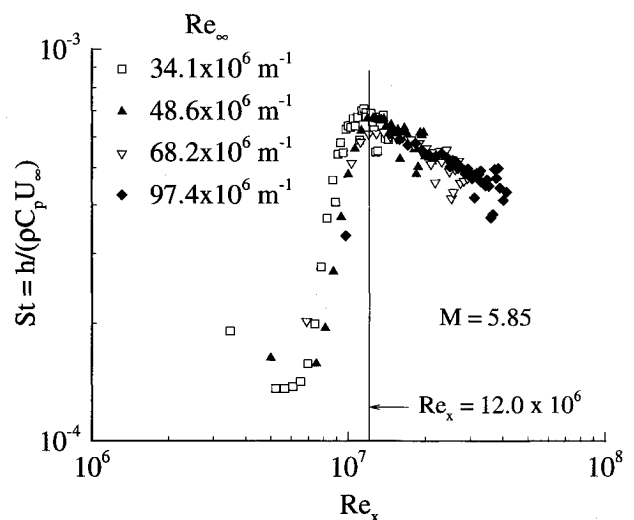


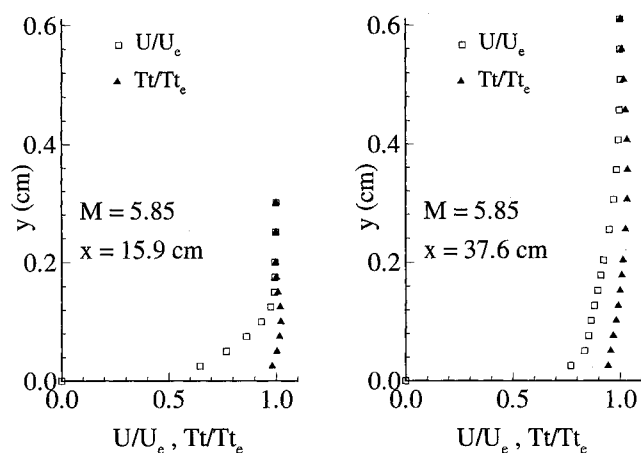
Fig. 2 Flat plate St distributions as a function of Re .

Table 1 Axial locations of flat plate peak heat transfer

| $M = 5.07$ | | $M = 5.85$ | |
|---------------------|--------------|--------------------|--------------|
| Re, m^{-1} | x_{tr}, cm | Re, m^{-1} | x_{tr}, cm |
| 45.9×10^6 | 23.9 | 34.1×10^6 | 31.7 |
| 65.6×10^6 | 17.3 | 48.6×10^6 | 25.7 |
| 92.2×10^6 | (12.1) | 68.2×10^6 | 18.9 |
| 131.6×10^6 | (8.5) | 97.4×10^6 | (12.3) |

Table 2 Boundary-layer thicknesses for Mach numbers 5.07 and 5.85

| $M = 5.07, Re = 65.6 \times 10^6 m^{-1}$ | | | $M = 5.85, Re = 48.6 \times 10^6 m^{-1}$ | | |
|--|--------------|-----------------------|--|-----------------------|--|
| x, cm | δ, cm | θ_m, cm | δ, cm | θ_m, cm | |
| 16.5 | 0.23 | 6.76×10^{-3} | 0.23 | 8.33×10^{-3} | |
| 34.3 | 0.46 | 1.46×10^{-2} | 0.57 | 1.67×10^{-2} | |
| 37.6 | 0.53 | 1.80×10^{-2} | 0.57 | 1.98×10^{-2} | |

Fig. 3 Velocity and total temperature profiles, transition-end at $x = 25.7$ cm.

determine the boundary-layer thickness (δ taken at $0.99\rho_e U_e$), in the SWBLI region; a constant value was assumed in this axial range (25–40 cm) since previous tests in this facility, with similar flat plate models,¹³ have shown that δ varies less than 10% over this short distance for unit Reynolds numbers ranging from $34.1 \times 10^6 m^{-1}$ to $98.4 \times 10^6 m^{-1}$. For this study, $\delta = 0.6$ cm for $M = 5.85$ and $\delta = 0.5$ cm for $M = 5.07$. Table 2 shows the measured values of both boundary-layer and momentum thickness for three axial locations and both Mach numbers of interest.

Flat Plate/Shock-Generator

Shock-generator angle, rather than static pressure rise, is employed as the ordinate since the angle is the geometric design parameter of interest here. Shock-generator angles associated with incipient separation were determined for more than 50 runs comprising this study by identifying a kink, or inflection point, in the axial pressure distribution. An example of this technique, first described by Kuehn¹⁴ and well-documented in the technical literature, is provided in Fig. 4. In Fig. 4, the incipient separation angle would be defined as the value halfway between 9.81 deg (angle for which the kink is first observed) and 9.24 deg (angle at which the kink disappears), i.e., 9.53 ± 0.3 deg. (Increments shown in θ are 0.6 deg in Fig. 4 for illustration only; an increment in θ of 0.2 deg was used for the study giving an uncertainty of ± 0.1 deg.) Although other techniques are available, the present authors chose this method for its convenience, repeatability, and practicality, the latter related to the fact that pressure taps are

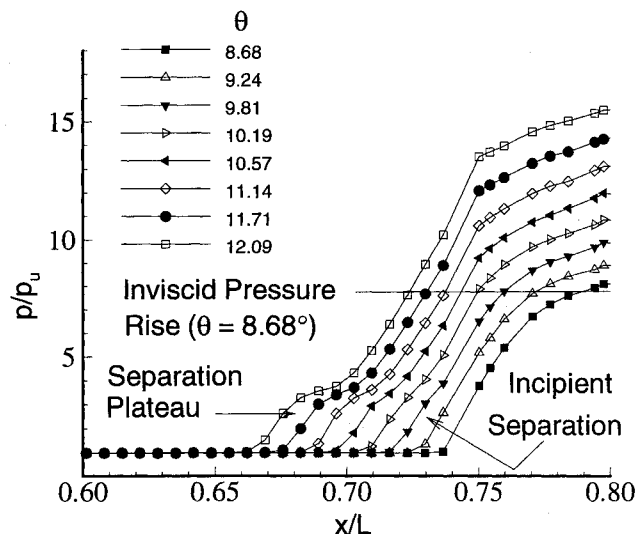


Fig. 4 Illustration of kink approach to determine incipient separation.

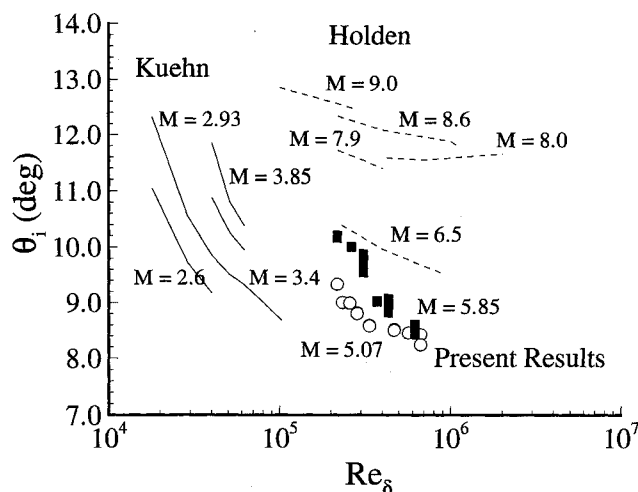


Fig. 5 Comparison of incipient separation results.

the most likely diagnostic to be used in the high-speed vehicle control systems related to the present effort.

Figure 5 compares the present incipient separation results to a selected portion of the historical database,^{4,14,15} in the format suggested by Kuehn. For those data associated with compression ramp configurations, inviscid oblique-shock relations were used to transform the ramp separation angles to equivalent (i.e., same static pressure rise) shock-generator angles. The two comparative databases shown were selected primarily because they include a relatively large range of both Mach and Reynolds numbers, thus allowing trends to be observed. In addition, both Kuehn's and Holden's data were obtained via the kink method (Holden utilized skin-friction gauges rather than pressure taps) and both investigators employed two-dimensional geometries. Of course, use of two-dimensional geometries do not imply two-dimensional flow. Both Holden and Kuehn claimed to have established two-dimensional flow with side plates (flow fences). Two dimensionality of the pressure test was verified through spanwise heat transfer gauges, pressure taps, and pitot pressure profiles.

It is seen that our results are reasonably consistent with Holden's over a similar Re_δ range. The θ_i uncertainty for our data is ± 0.4 deg, a number representing the uncertainty in shock-generator angle, the run-to-run repeatability, and the definition of incipient separation given previously. As Re_δ

increases, the θ_i values are seen to decrease. For our data, this is believed to be associated with the proximity of the SWBLI to the transition-end location. The reasoning here is that the boundary layer is somehow "stronger" (i.e., more resistant to separation) at SWBLI locations close to the transition-endpoint than it is in the fully turbulent region. This assumption can be justified as follows.

As an example, say that the boundary-layer velocity profile can be described in terms of a power-law function, that is $U/U_\infty = (y/\delta)^{1/N}$. For fully turbulent flows, $N = 7$ is typically used. Johnson and Bushnell⁸ presented an extensive amount of flat plate, cone, hollow cylinder, and nozzle-wall data clearly showing that N can rise to more than double this value at short distances downstream of the peak-heating location. This phenomenon was described as an "overshoot" of the power-law exponent. Although reasons for this overshoot were not discussed in detail, the present authors believe that it may be related to a high degree of mixing (a remnant of the boundary-layer transition) in the boundary layer in the neighborhood of the transition-endpoint. The mixing would likely reduce the size of the laminar sublayer, which, according to Holden,¹⁵ is where a shock-induced separation is initiated. Thus, SWBLI locations close to the transition-endpoint are associated with larger shock-induced pressure rises, before separation is observed, than are SWBLI locations far downstream of the transition-endpoint.

The decrease in the incipient separation angle as Re_δ is increased (for $Re_\delta < 10^6$ in Fig. 5) can be explained in terms of this overshoot. Consider that Re_δ can be increased by raising the unit Reynolds number (the corresponding change in δ is ignored for the present). As unit Reynolds number increases, the transition-endpoint moves forward (on a flat plate) and since the SWBLI location is relatively insensitive to Reynolds number, the proximity of the SWBLI with respect to the end of transition increases. Alternatively, one could raise Re_δ by increasing δ , for a fixed unit Reynolds number. This would be accomplished by increasing the flat plate length, but this also results in an increase between the end of transition and the SWBLI location as long as the shock-generator position stays fixed.

A third method of increasing the local Reynolds number is by tilting the flat plate as in the present study. Although this decreases δ relative to the untilted plate, the transition-endpoint is moved far forward, and thus, $x_s - x_{tr}$ is increased, which allows the power-law exponent to relax to a "fully turbulent" value (the boundary-layer strength diminishes), thus resulting in lower incipient separation angles. Figure 6 is a plot of our incipient separation data as a function of

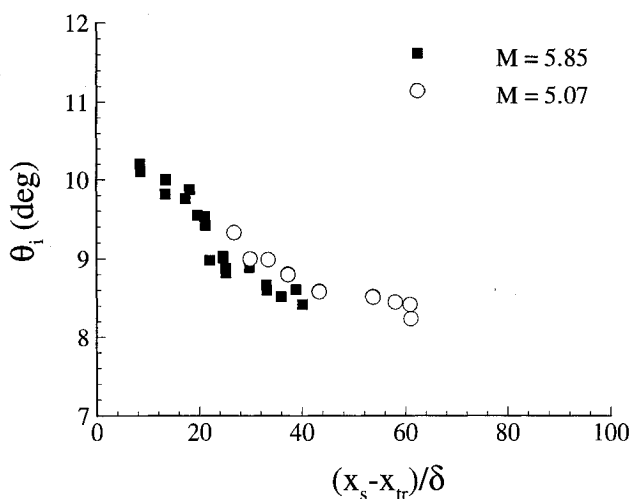


Fig. 6 Incipient separation results showing the influence of the distance between the SWBLI and the transition-end location.

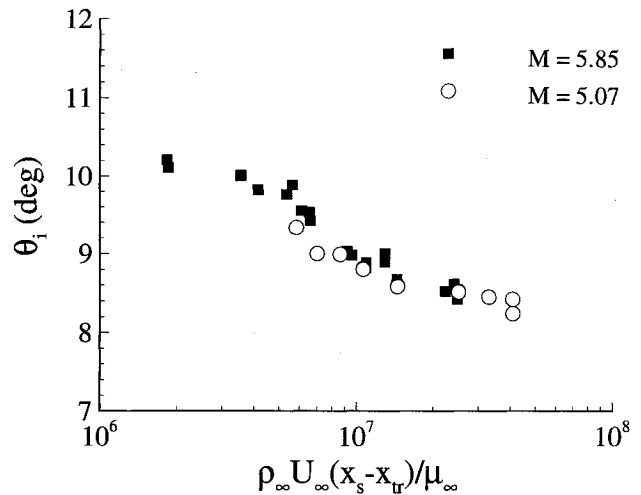


Fig. 7 Alternative plotting of Fig. 6.

proximity to transition-end normalized by the local boundary-layer thickness. It is seen that a distance of about 50δ downstream from the peak heating location is required before we observed the fully turbulent SWBLI (the incipient separation angle becomes a constant ~ 8.4 deg). This value (50δ) is in agreement with that suggested by Johnson and Bushnell's correlations. Ours is not a unique explanation for the decrease of θ_i as Re_δ increases (e.g., Ref. 15), but we do believe this is the first time data are being presented that quantify the incipient separation angle as a function of proximity to the transition-endpoint.

Unfortunately, this type of plot is not common in the literature. This makes the comparison of incipient separation data from various investigators difficult. Such information would help to clarify the role of δ , e.g., as an independent variable in incipient separation, by allowing the transition influence to be discounted in certain database comparisons. This δ influence becomes an important concern when one wishes to scale incipient separation data from wind-tunnel models to full-scale flight vehicles.

An interesting trend observed for the current test involving incipient separation is depicted in Fig. 7. Here, θ_i is plotted as a function of a Reynolds number based on the distance between transition-end and the inviscid shock impingement location; $Re_{x_{tr}} = Re_x \cdot (x_s - x_{tr})$, where Re_x is the unit Reynolds number.

Although unorthodox, it is seen that incipient separation becomes more a function of transition location and Reynolds number than a function of Mach number (at least over this small Mach number range). Since accurate transition location data is not typically included in the SWBLI literature, application of this technique to other data sets and, hence, other Mach numbers is presently impossible. Whether this trend will continue over a greater Mach number range is unknown, but this emphasizes the need for SWBLI investigators to be complete in the reporting of test parameters, particularly transition start and end locations.

References

- ¹Roshko, A., and Thomke, G. J., "Supersonic, Turbulent Boundary Layer Interaction with a Compression Corner at Very High Reynolds Number," *Proceedings of the Supersonic and Hypersonic Flow (AD 714362)*, Hypersonic Research Lab., Wright-Patterson AFB, OH, 1970, pp. 109-138; also McDonnell Douglas Aircraft Co. Rept. 10163, May 1969.
- ²Coleman, G. T., Elfstrom, G. M., and Stollery, J. L., "Turbulent Boundary Layers at Supersonic and Hypersonic Speeds," Symposium on Turbulent Shear Flows, AGARD CP 93, Paper 31, 1971.
- ³Elfstrom, G. M., "Turbulent Hypersonic Flow at a Wedge

Compression Corner," *Journal of Fluid Mechanics*, Vol. 53, Pt. I, 1972, pp. 113-127.

⁴Holden, M. S., "Shock Wave—Turbulent Boundary Layer Interaction in Hypersonic Flow," AIAA Paper 72-74, Jan. 1972.

⁵Appels, C., and Richards, B. E., "Incipient Separation of a Compressible Turbulent Boundary Layer," Von Kármán Inst. for Fluid Dynamics, TN 99, Belgium, 1974.

⁶Settles, G. S., Bogdonoff, S. M., and Vas, I. E., "Incipient Separation of a Supersonic Turbulent Boundary Layer at High Reynolds Number," *AIAA Journal*, Vol. 14, No. 1, 1976, pp. 50-56.

⁷Delery, J., and Marvin, J. G., *Shock Wave Boundary Layer Interactions*, edited by Eli Reshotko, AGARDograph 280, Feb. 1986.

⁸Johnson, C. B., and Bushnell, D. M., "Power-Law Velocity Profile Exponent Variation with Reynolds Number, Wall Cooling and Mach Number in a Turbulent Boundary Layer," NASA TN D-5753, April 1970.

⁹Reda, D. C., and Murphy, J. D., "Shock Wave/Turbulent Boundary Layer Interactions in Rectangular Channels," *AIAA Journal*, Vol. 11, No. 2, 1973, pp. 139, 140.

¹⁰Reda, D. C., and Murphy, J. D., "Sidewall Boundary Layer

Influence on Shock Wave/Turbulent Boundary Layer Interactions," *AIAA Journal*, Vol. 11, No. 10, 1973, pp. 1367, 1368.

¹¹Frew, D. R., Galassi, L., Stava, D. J., and Azevedo, D., "A Study of Incipient Separation Limits for Shock-Induced Boundary Layer Separation for Mach 6 High Reynolds Flow," AIAA Paper 93-2481, June 1993.

¹²Molten, R. G., "Expansion of the Aerodynamic Simulation Capabilities of the Air Force WRDC Mach 6 High Reynolds Number Facility," Wright Research and Development Center, WRDC-TM-89-173-FIMG, Wright-Patterson AFB, OH, Aug. 1989.

¹³Galassi, L., and Scaggs, N., "Experimental and Computational Comparisons of Mach 6 High Reynolds Number Heat Transfer and Skin Friction," Fluid Dynamics Panel Symposium, AGARD Paper 21, Torino, Italy, May 1992.

¹⁴Kuehn, D. M., "Experimental Investigation of the Pressure Rise Required for the Incipient Separation of Turbulent Boundary Layer in Two Dimensional Supersonic Flow," NASA Memo 1-21-59A, Feb. 1959.

¹⁵Holden, M. S., "Shock Wave-Turbulent Boundary Layer Interaction in Hypersonic Flow," AIAA Paper 77-45, Jan. 1977.